Phase Shift Optimization for RIS Element-Based Index Modulation

1st Krisma Asmoro
Dept. of IT Convergence Engineering
Kumoh National Institute of Technology
Gumi, South Korea
krisma@kumoh.ac.kr

2nd Soo Young Shin
Dept. of IT Convergence Engineering
Kumoh National Institute of Technology
Gumi, South Korea
wdragon@kumoh.ac.kr

***Abstract*—This study investigates a phase shift optimization of reconfigurable intelligent surface (RIS) element-based index modulation (IM). The RIS-based IM employs the spatial modulation (SM) technique, which utilizes active indices of RIS elements as additional bits. Therefore, it can enhance bits per channel usage (BPCU) for each user with lower modulation. However, due to the user's mobility and RIS hardware limitation, it is challenging to determine the phase shifter of RIS elements. This study formulates a non-convex problem to decrease symbol error rate (SER) by maximizing the minimum Euclidian distance. The successive convex approximation algorithm is adopted in this study to obtain an approximate optimal solution for RIS phase shifter. The computer simulation result shows that the RIS-based IM could enhance BPCU. In addition, it has a lower SER than SM-based transmission without RIS.**

***Index Terms*—non-convex optimization, reconfigurable intelligent surfaces (RIS), spatial modulation (SM), symbol error rate (SER).**

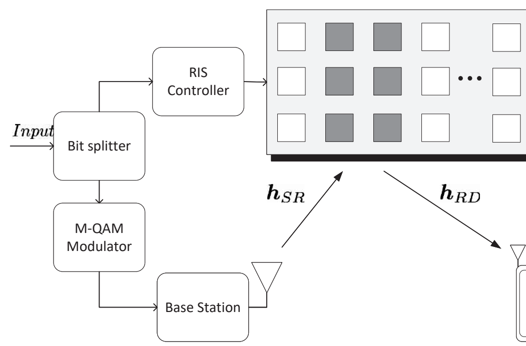

Fig. 1. System model of RIS-based index modulation.

I. Introduction

Reconfigurable intelligent surfaces (RIS) recently emerged as a potential technology to support beyond 6G wireless communication [1]. The RIS is recently gaining popularity as a research direction because of its backward compatibility for 5G technology and potentially fulfilling beyond 6G communication that requires massive coverage [2]. The RIS consists of several reflecting elements that can be tuned electrically to control the propagation channel [3]. The low-cost elements of RIS mainly focus on manipulating phase shift and amplitude of the incident signal; thus, it is different from the relay, where its capability of amplifying and decoding an incoming signal [4]. However, due to hardware limitations, RIS can not perfectly manipulate an incident signal to the users. Therefore, several studies proposed a RIS phase shifter optimization algorithm to maximize sum-rate capacity [5], energy efficiency [6], and SER [7] in a multiple-input-multiple-output (MIMO) system.

Spatial modulation (SM) is a well-known technique to provide better spectral efficiency (SE) and implementation cost of MIMO systems [8]. The spatial modulation technique employs a bit splitter to divide incoming bits into spatial bits and amplitude phase modulation (APM). Further, the spatial bits act as an activator to activate a single or one group of antennas. Then, the transmitted symbol contains an index of an active antenna and APM symbols. As a result, users can jointly decode an incoming symbol to detect spatial bits and modulated APM bits. Therefore, with a spatial signal constellation, the system can increase bits per channel usage (BPCU) and reduce symbol error rates (SER). Motivated by these benefits, the SM technique is integrated with RIS to provide better SE and SER [9].

Motivated by RIS-based index modulation, this study proposed an algorithm to optimize the RIS phase shifter. In contrast with existing literature that optimizes RIS based on sum rate and SE, this study aims to minimize SER. This study first observes the maximum likelihood (ML) detector and then proposes a solution to maximize an Euclidian distance for every symbol error. In addition, as this study considers discrete phase shifter optimization for a practical approach, the phase shift optimization becomes an np-hard problem and non-convex. Thus this study formulates a non-convex optimization problem and proposes successive convex approximation (SCA) to obtain a near-optimal solution.

II. System Model

A. RIS-based Index Modulation

Consider downlink scenario RIS-based IM transmission with a single antenna base station (BS) and an arbitrary number of receiver antenna N_r, depicted in Fig. 1. The RIS is equipped with N number of elements, and every element is controlled with a field programmable array (FPGA) linked with BS. Further, BS will cooperate with FPGA to control which RIS elements need to be activated according to the user symbol. The main function of RIS is to reflect incoming signals to users by tuning its phase shift. Denotes phase shifter vector array as $\mathbf{\Phi} = \text{diag}\{\Lambda_1 e^{\varphi_1}, \cdots, \Lambda_i e^{\varphi_i}, \cdots \Lambda_N e^{\varphi_N}\}$, where Λ_i, φ_i denotes amplitude and phase shift of i-th element, respectively. Considering the practicality of the proposed system, this study utilizes a discrete phase shifter with parameter D_φ as the integer number of bits used per element [10]. Therefore, the value of phase shifter can be written as $\varphi_i \in \Theta = \left[0, \frac{2\pi}{2^{D_\varphi}}, \cdots, \frac{2\pi(2^{D_\varphi - 1})}{2^{D_\varphi}}\right]$. The discrete value of Θ is assumed to be equally spaced in $[0, 2\pi)$.

Based on Fig. 1, the incoming user bits with BPCU $log_2(M) + log_2(N)$ are split into two. The first $log_2(M)$ bits will go to amplitude-phase modulation (APM), and the remaining $log_2(N)$ will be utilized as activation index. The output of APM is a modulated symbol, selected from its constellation $S_m \in [\mathcal{S}_1, \mathcal{S}_2, \cdots, \mathcal{S}_M]$, while the index activator is $\ell \in [1, \cdots, N]$. Therefore, the transmitted signal is written as:

$$x_t^{RF}(t) = \underbrace{[0 \ \cdots \ \mathcal{S}_m \ \cdots 0]}_{N}{}^{T}. \tag{1}$$

Consider N_r antenna at the receiver, the received signal at the user is $\boldsymbol{Y} = [y_1, \cdots, y_r, \cdots, y_{Nr}]$. Furthermore with the predefined $\mathbf{\Phi}$, it can be written as:

$$\boldsymbol{Y} = \boldsymbol{h_{SR}} \mathbf{\Phi} \boldsymbol{h_{RD}} x + \boldsymbol{n}, \tag{2}$$

where $\left[\boldsymbol{h_{SR}} \in \mathbb{C}^{N \times 1}, \boldsymbol{h_{RD}} \in \mathbb{C}^{N_r \times N}\right]$ following Rayleigh fading channel $\sim \mathcal{CN}\left(0, \sigma^2\right)$. $\boldsymbol{n}$ denotes additive white Gaussian noise (AWGN) that follows distribution $\sim \mathcal{CN}\left(0, \sigma^2 \mathbf{I}_{Nr}\right)$.

B. Maximum Likelihood Detector

On the receiver side, the maximum-likelihood (ML) detector is applied to recover the transmitted signal $\mathcal{S}_{\tilde{m}}$ and index $\tilde{\ell}$, and it can be written as:

$$[\tilde{\ell}, \tilde{m}] = \underset{\ell, x}{\arg\min} \left\| \mathbf{Y} - \underbrace{\boldsymbol{h_{SR}} \mathbf{\Phi} \boldsymbol{h_{RD}}}_{\mathbf{H}_\ell} x \right\|_F^2, \tag{3}$$

where $\mathbf{H} \in \mathbb{C}^{N_r \times N}$ denotes the overall channel of selected index ℓ. The $\|\cdot\|_F$, Frobenius norm is utilized because of Nr number of a received signal.

The ML detector performs an exhaustive search through all candidates that jointly decode the active RIS index $\tilde{\ell}$ and modulated symbol $\tilde{m}$. Based on the given ML detector, the pairwise error probability (PEP) bound can be approximated as [11], [12]:

$$\begin{aligned} &\mathrm{P_e} = \Pr\left((\ell, x) \to (\tilde{\ell}, \tilde{x}) \mid \mathbf{h_{SR}}, \mathbf{h_{RD}}\right) \\ &\mathrm{P_e} \leq Q\left(\sqrt{\frac{\left\|\mathbf{H}_\ell x - \mathbf{H}_{\tilde{\ell}} \tilde{x}\right\|_\mathrm{F}^2}{2\sigma_n^2}}\right) = Q\left(\sqrt{\frac{v_{\ell, \tilde{\ell}}^{m, \tilde{m}}}{2\sigma_n^2}}\right), \end{aligned} \tag{4}$$

where σ_n^2 is AWGN noise, $Q(\cdot)$ denotes a q-function that is written as $Q(x) = \frac{1}{\sqrt{2\pi}} \int_x^\infty \exp\left(-\frac{u^2}{2}\right) du$, while $v_{\ell, \tilde{\ell}}^{m, \tilde{m}}$ denotes minimum squared euclidean distance. Assuming perfect channel state information (CSI) we can simplify the ML detector as:

$$v_{min}(\mathbf{\Phi}) = \arg\ \min \|\boldsymbol{h_{SR}} \mathbf{\Phi} \boldsymbol{h_{RD}} (x - \tilde{x})\|_{\forall m, \ell \neq \tilde{m}, \tilde{\ell}}. \tag{5}$$

Based on Eq. (5), the minimum Euclidian distance is based on the given phase shift. Therefore, in this study, we denote a minimum Euclidian distance with a given phase shifter $\mathbf{\Phi}$ with $v_{min}(\mathbf{\Phi})$.

III. RIS Phase Shift Design

A. Problem Formulation

Based on given Eq. (5), it can be observed that the problem is considered as NP-hard and non-convex. In addition, it is challenging to model phase shifter optimization based on symbol error rate (SER) approximation. Therefore, we adopt problem formulation based on maximize minimum Euclidian distance (MMED) [12], [13] to determine RIS phase shifter. The problem formulation of the proposed system can be written as:

$$\begin{aligned} \max_{\mathbf{\Phi}} \quad & \min_{\forall (m, \ell) \neq (\tilde{m}, \tilde{\ell})} \|\boldsymbol{h_{SR}} \mathbf{\Phi} \boldsymbol{h_{RD}} (x - \tilde{x})\| \\ \text{s.t.} \quad & \mathbf{v}[n] \in \Phi, \quad n = 1, 2, \cdots, N. \end{aligned} \tag{6}$$

B. Iterative based approximation

To deal with the presented non-convex problem, this study proposed an iterative penalty-based algorithm to approximate the solution. In particular, it is challenging to handle discrete phase shifter $e^{j\varphi_i}$. Therefore, we introduce vector $\boldsymbol{\beta} = [b_1, \cdots, b_i, \cdots, b_N]$ that contains RIS phase shifter and it holds $\boldsymbol{\beta} = \mathbf{\Phi}$. Furthermore, the problem can be transformed into an equivalent form:

$$\begin{aligned} \max_{\mathbf{\Phi}} \quad & v_{min}(\mathbf{\Phi}) - \lambda \|\mathbf{\Phi} - \boldsymbol{\beta}\|^2 \\ \text{s.t.} \quad & b_i \in \mathbf{\Theta}, \quad i = 1, 2, \cdots, N. \end{aligned} \tag{7}$$

where λ is a positive integer value that denotes penalty variable for penalizing the violation of equality constraint. In this study, Eq. (7) will be solved for P iteration and λ will be updated with $\lambda = Z\lambda$ (Z is a sufficiently large positive constant, e.g., $Z > 1$). It can be seen that by increasing the value of λ, maximizing the objective function, approximately $\boldsymbol{\beta} \approx \mathbf{\Phi}$.

However, for a certain number of λ, it is still challenging to solve the problem. First, we rewrite RIS phase shift array from diagonal matrix $\mathbf{\Phi}$ to a non-diagonal matrix which is denoted as $\mathbf{\Gamma} \in \mathbb{C}^{N \times 1} = [\gamma_1, \cdots, \gamma_i, \cdots, \gamma_N]$. Further, Eq. (5) can be equally transformed as follows:

$$\begin{aligned} v_{min}(\mathbf{\Phi}) &= \min \|\boldsymbol{h_{SR}} \mathbf{\Phi} \boldsymbol{h_{RD}} (x_\ell^m - \tilde{x}_{\tilde{\ell}}^{\tilde{m}})\|^2 \\ &= \min \|(\boldsymbol{A}_\ell \mathbf{\Phi} \boldsymbol{G_\ell}) \mathcal{S}_m - (\boldsymbol{A}_{\tilde{\ell}} \mathbf{\Phi} \boldsymbol{G_\ell}) \mathcal{S}_{\tilde{m}}\|^2 \\ v_{min}(\mathbf{\Gamma}) &= \min \|(\boldsymbol{A}_\ell \boldsymbol{B}_\ell \mathbf{\Gamma}) \mathcal{S}_m - (\boldsymbol{A}_{\tilde{\ell}} \boldsymbol{B}_{\tilde{\ell}} \mathbf{\Gamma}) \mathcal{S}_{\tilde{m}}\|^2, \end{aligned} \tag{8}$$

where $\boldsymbol{A_\ell}$ and $\boldsymbol{G_\ell}$ denote ℓ column of $\boldsymbol{h_{SR}}$ and $\boldsymbol{h_{RD}}$, respectively. In addition, define diagonal matrix of $\boldsymbol{B_\ell}$ as $\text{diag}\{\boldsymbol{G_\ell}\}$. Furthermore, define $\boldsymbol{D}_{\ell, \tilde{\ell}}^{m, \tilde{m}} = \boldsymbol{A}_\ell \boldsymbol{B}_\ell \mathcal{S}_m -$

Algorithm 1 Algortihm for solving Eq. (11)

Initialize: $w = 0$, $\boldsymbol{J}_0$, L_0, $\boldsymbol{\Gamma}_0$, W, ε_{SCA}
while $w < W$ or $\|\boldsymbol{\Gamma_w} - \boldsymbol{\Gamma_{w+1}}\|^2 \leq \varepsilon_{SCA}$ **do**
  Update L_w and $\boldsymbol{J}_w$
  Update $\boldsymbol{\Gamma}_w$ by solving problem Eq. (11)
  $w \leftarrow w + 1$
end while
return $\boldsymbol{\Gamma}^*$

$\boldsymbol{A}_{\tilde{\ell}}\boldsymbol{B}_{\tilde{\ell}}\mathcal{S}_{\tilde{m}}$, then we can rewrite again the euclidian distance as:

$$\begin{aligned} v_{min}(\boldsymbol{\Gamma}) =& \min\|\boldsymbol{D}_{\ell,\tilde{\ell}}^{m,\tilde{m}}\boldsymbol{\Gamma}\|^2 \\ =& \min\{\boldsymbol{\Gamma}^H((\boldsymbol{D}_{\ell,\tilde{\ell}}^{m,\tilde{m}})^H\boldsymbol{D}_{\ell,\tilde{\ell}}^{m,\tilde{m}})\boldsymbol{\Gamma} + 2\Re\{\boldsymbol{D}_{\ell,\tilde{\ell}}^{m,\tilde{m}}\boldsymbol{\Gamma}\}\}, \end{aligned} \tag{9}$$

where $\Re\{\cdot\}$ denotes real part of complex value. The maximization problem Eq. (7) can be rewritten as follows:

$$\begin{aligned} \max_{\boldsymbol{\Gamma}} \quad & T_{\ell,\tilde{\ell}}^{m,\tilde{m}}(\boldsymbol{\Gamma}) \\ \text{s.t.} \quad & b_i \in \boldsymbol{\Theta}, \quad i = 1, 2, \cdots, N. \end{aligned} \tag{10}$$

where $T_{\ell,\tilde{\ell}}^{m,\tilde{m}} = v_{min}(\boldsymbol{\Gamma}) - \lambda\|\boldsymbol{\Gamma} - \boldsymbol{\beta}\|^2$. It can be observed that $T_{\ell,\tilde{\ell}}^{m,\tilde{m}}$ is not convex, although $v_{min}(\boldsymbol{\Gamma})$ and $\|\boldsymbol{\Gamma} - \boldsymbol{\beta}\|^2$ are convex functions. Therefore, in this study, we utilize successive convex approximation (SCA) to approximate the value of $T_{\ell,\tilde{\ell}}^{m,\tilde{m}}$. The function $\boldsymbol{\Gamma}^H((\boldsymbol{D}_{\ell,\tilde{\ell}}^{m,\tilde{m}})^H\boldsymbol{D}_{\ell,\tilde{\ell}}^{m,\tilde{m}})\boldsymbol{\Gamma}$ can be approximated by using first-order Taylor expansion. Denotes w as the feasible point, then we can reformulate Eq. 7 as:

$$\begin{aligned} \max_{\boldsymbol{\Gamma}} \quad & \min\{2\Re\{\boldsymbol{J}_w\boldsymbol{\Gamma}\} + L_w - \lambda\|\boldsymbol{\Gamma} - \boldsymbol{\beta}\|^2\}, \\ \text{s.t.} \quad & b_i \in \boldsymbol{\Theta}, \quad i = 1, 2, \cdots, N. \end{aligned} \tag{11}$$

where $\boldsymbol{J}_w = \boldsymbol{D}_{\ell,\tilde{\ell}}^{m,\tilde{m}} + \boldsymbol{\Gamma}_w^H((\boldsymbol{D}_{\ell,\tilde{\ell}}^{m,\tilde{m}})^H\boldsymbol{D}_{\ell,\tilde{\ell}}^{m,\tilde{m}})$ and $L_w = -\boldsymbol{\Gamma}_w^H((\boldsymbol{D}_{\ell,\tilde{\ell}}^{m,\tilde{m}})^H\boldsymbol{D}_{\ell,\tilde{\ell}}^{m,\tilde{m}})\boldsymbol{\Gamma}_w$. It can be seen that $-\lambda\|\boldsymbol{\Gamma}-\boldsymbol{\beta}\|^2$ is a concave function of the phase shifter. In addition, $2\Re\{\boldsymbol{J}_w\boldsymbol{\Gamma}\}$ is a linear function, hence Eq. (11) is convex. Specifically, the problem shown in Eq. (11) can be solved efficiently with CVX discipline programming [14], [15].

C. Algorithm for Maximizing Minimum Euclidian Distance

To solve Eq. (11), we utilize maximum iteration that is denoted by W and ε_{SCA} being a small threshold, e.g. 0,0001. The SCA algorithm could optimize $\boldsymbol{\Gamma}^*$ at a given random value of $\boldsymbol{\Gamma}_0$. In addition, SCA algorithm works by fixing $\boldsymbol{\beta}$ and $L_w, \boldsymbol{J}_w$ obtained from $\boldsymbol{\Gamma}_{w-1}$ denotes phase shift previous iteration.

The output value of $\boldsymbol{\Gamma}^*$ the Algorithm 1 is still a continuous phase shifter. Therefore, by fixing the value of $\boldsymbol{\Gamma}$, the problem Eq. (7) can be alternated to:

$$\begin{aligned} \max_{\boldsymbol{\beta}} \quad & v_{min}(\boldsymbol{\Gamma}) - \lambda\|\boldsymbol{\Gamma}^* - \boldsymbol{\beta}\|^2 \\ \text{s.t.} \quad & b_i \in \boldsymbol{\Theta}, \quad i = 1, 2, \cdots, N. \end{aligned} \tag{12}$$

Furthermore, by fixing the value of penalty constraint λ, the problem formulation (12) can be decoupled as follows:

Algorithm 2 Algorithm for solving Eq. (7)

Initialize: $c = 0$, C, λ, Z, $\boldsymbol{\Gamma}_0$, $\boldsymbol{\beta}_0$, ε_P
  Initialisation : $\lambda = 1$, $\boldsymbol{\beta}_0 = \boldsymbol{\Gamma}_0$
while $c < C$ or $\|\boldsymbol{\Gamma}^* - \boldsymbol{\beta}^*\| \leq \varepsilon_P$ **do**
  Assign phase shifter value $\Gamma_w = \boldsymbol{\Gamma}_c$
  Update the value of RIS phase shifter which obtained from Algorithm 1 ($\boldsymbol{\Gamma}_{c+1} = \boldsymbol{\Gamma}_w^*$)
  Update value $\boldsymbol{\beta}^*$ by solving Eq. (12)
  $\lambda \leftarrow Z\lambda$
  $c \leftarrow c + 1$
end while
return $\boldsymbol{\beta}^*, \Gamma^*$

$$\begin{aligned} \min_{\boldsymbol{\beta}} \quad & \|\boldsymbol{\Gamma}^* - \boldsymbol{\beta}\|^2 \\ \text{s.t.} \quad & b_i \in \boldsymbol{\Theta}, \quad i = 1, 2, \cdots, N. \end{aligned} \tag{13}$$

Thus, it can be seen that $\boldsymbol{\beta}$ is decoupled from the function, and solving b_i can be done by finding the closest point from $\varphi_i \in \boldsymbol{\Theta}$ to $\gamma_i \in \boldsymbol{\Gamma^*}$. Denotes the phase of b_i as $\tilde{\varphi}_i$, then it can be written as follows:

$$b_i = e^{j\tilde{\varphi}_i}, \ \tilde{\varphi}_i = \arg\min|\angle\{\gamma_i\} - \varphi_i|, \tag{14}$$

where $\angle\{\cdot\}$ denotes an angle operator that obtain phases from optimized variable $\gamma_i \in \boldsymbol{\Gamma}^*$.

To solve Eq. (7), penalty iterative Algorithm 2 is proposed. The proposed algorithm will iteratively approximate the solution of discrete phase shifter $e^{j\varphi_i}$ by solving Algorithm 1 (with fixed λ, $\boldsymbol{\beta}$). Afterwards, Eq. (14) is estimated by fixing λ and $\boldsymbol{\Gamma}^*$. Then, λ will be updated with Z being a positive constant real value, resulting in λ increasing each iteration c. In this study, the convergence criterion fulfills when $\|\boldsymbol{\Gamma}^* - \boldsymbol{\beta}^*\| < \varepsilon_P$, where ε_P denotes a sufficiently small constant value.

IV. Performance Result and Analysis

In this study, we test the proposed algorithm with computer simulation. For SCA-based approximation and penalty iterative algorithm, this study follows parameter simulation in Table I. It can be seen clearly that for each iteration in Algorithm 2, value of λ becomes larger, i.e. $(1, 10^1, 10^2, \cdots, 10^C)$. At the same time, the value of $\|\boldsymbol{\Gamma}^* - \boldsymbol{\beta}^*\|$ is getting smaller and asymptotically approaches 0 as the iteration increases. Therefore, λ acts as a variable to scale up the penalty terms $\|\boldsymbol{\Gamma}^* - \boldsymbol{\beta}^*\|$ and force the problem Eq. (7) to converge at local optimum. Thus, it can be concluded that the lower value of penalty terms, better solution of the discrete phase shifter.

Fig. 2 shows the BER performance of different system models. Specifically, this result employs additional parameters as follows: $N = 20$, $D_\varphi = 4$, $\sigma_n \in [-15, -13, \cdots, 15]dB$. It can be seen that the proposed system outperforms conventional spatial modulation [8]. Targeting BER below 10^{-3}, the proposed algorithm could achieve it $\approx 6dB$ lower than the conventional SM. On the other hand, in comparison with the ideal continuous RIS phase shifter [11], the system requires $\approx 8dB$ to achieve 10^{-3} BER.

TABLE I
COMPUTER SIMULATION PARAMETER VALUE

Parameter	Value
SCA Iteration (W)	10
Threshold SCA (ε_{SCA})	10^{-3}
Penalty iterative Iteration (C)	8
Threshold penalty iterative (ε_P)	10^{-5}
Initial penalty value (λ)	1
Update penalty value (Z)	10
RIS sub-group element (N_t)	4
Receive antenna (N_r)	4

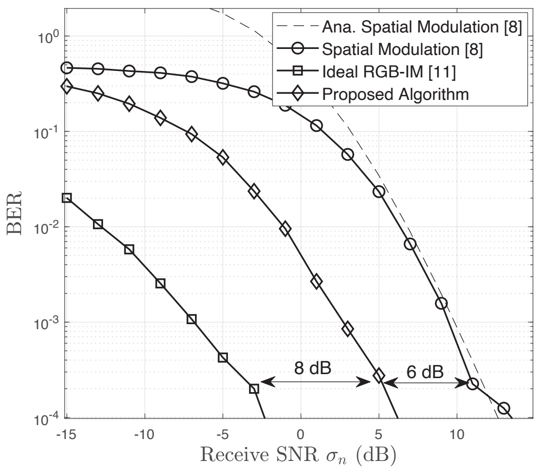

Fig. 2. BER comparison of the proposed algorithm with an existing model.

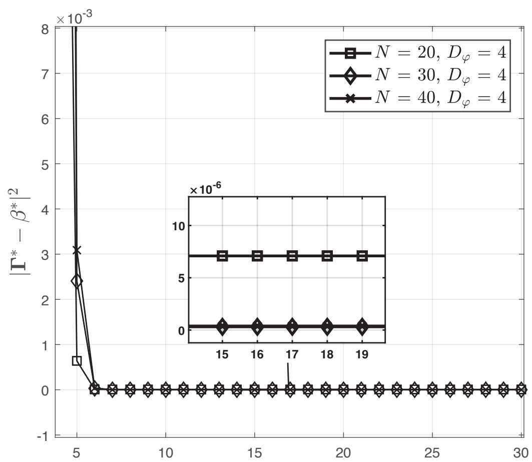

Fig. 3. Penalty value over a different number of elements.

Further, to inspect the impact of the iteration number with respect to the penalty variables, this study plots the value of $\|\mathbf{\Gamma}^* - \boldsymbol{\beta}^*\|$ with iteration C ranging from 1 to 30. The Fig. 3 depicts a comparison of different numbers of elements with $N \in [20, 30, 40]$ with the same discrete bits phase shifter $D_\varphi = 4$. For a low number of iterations, all elements are converged at $c > 5$. However, a different trend was

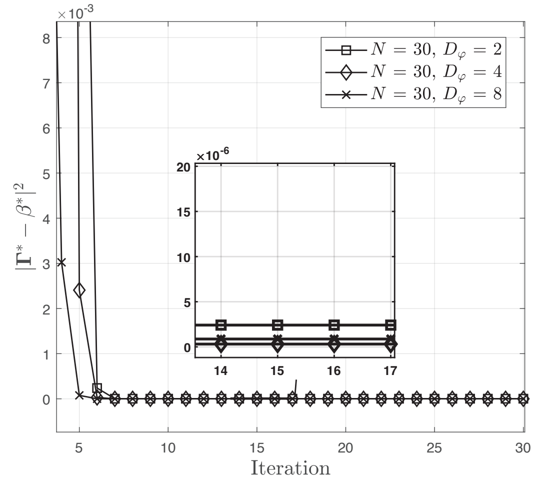

Fig. 4. Penalty value over a different number of bits of discrete phase shifter.

shown on a higher number of iterations. It is shown that the number of elements $N = 20$ resulting in the penalty value is $\approx 5 \times 10^{-6}$, while the other elements are below $\approx 10^{-6}$. From the magnifier plot, it can be seen that the lower element number can potentially lead to a non-optimal solution. In addition, the figures show that the limitation of the current algorithm could approximate the optimal discrete phase shifter for higher elements.

Fig. 4 depicts the impact of different numbers of phase shifter bits with penalty variables. In this figure, the number of elements is similar, while the number of bits for the discrete phase shifter is $D_\varphi \in [2, 4, 8]$. For small number of c, it can be seen clearly that $D_\varphi = 8$ converges faster than $D_\varphi \in [2, 4]$. Moreover, for $c < 4$, the value of lower bits of discrete phase shifter results in a very high penalty value. In addition, for a higher value of c, $D_\varphi = 2$ results in more penalty variables than the other bits. From the magnifier plot, it can be seen that the lower element number can potentially lead to a non-optimal solution.

To conclude, the presented computer simulation result of this study. Several analyses conclude that RIS based-IM has the potential to fulfill the demand of 6G or beyond 6G communication is described as follows:

- The proposed RIS-based IM can enhance BPCU and SE by adding additional spatial bits to user bits as an activator of elements;
- This study proposed a discrete RIS phase shifter, which is more applicable for hardware realization since continuous phase shifter is difficult to design;
- Based on the simulation, the classical optimization algorithm can achieve a convergence state with a low number of iterations, reducing computational complexity.

However, despite the numerous advantages of the proposed RIS-based IM, it had a major drawback. In comparison with RIS-assisted communication, RIS-based IM achieves a higher SER. This is because the RIS-based IM requires to turn off several elements in order to work. Therefore, RIS-assisted communication had a better SER because the elements is fully activated, but it has a lower BPCU.

V. CONCLUSION

This study offers a more realistic approach to RIS-based index modulation with a non-convex optimization technique. Moreover, this study considers discrete phase shifters to mitigate implementation issues. The computer simulation shows that the proposed algorithm can outperform conventional spatial modulation with a similar number of receive antenna and spatial bits. Therefore, it can be exploited for beyond 6G communication as it demands high SE and reliability. In addition, in beyond 6G communication, RIS-based IM can enhance BPCU and cover more area than conventional SM. Moreover, this study observes and analyzes the impact of number iteration with the penalty function value. It can be concluded that a lower number of bits to generate a discrete phase shifter can lead to slower convergence. However, with higher bits and RIS elements, the proposed algorithm gains the benefit of requiring a sufficiently small number of iterations to converge. Future studies will address the impact of imperfect CSI and BS precoding optimization.

ACKNOWLEDGEMENT

This research was supported by the MSIT(Ministry of Science and ICT), Korea, under the Innovative Human Resource Development for Local Intellectualization support program (IITP-2023-2020-0-01612) supervised by the IITP(Institute for Information communications Technology Planning Evaluation) and by Basic Science Research Program through the National Research Foundation of Korea(NRF) funded by the Ministry of Education(No. 2022R1I1A1A01069334)

REFERENCES

[1] E. Basar, M. Di Renzo, J. De Rosny, M. Debbah, M. Alouini, and R. Zhang, "Wireless communications through reconfigurable intelligent surfaces," *IEEE Access*, vol. 7, pp. 116 753–116 773, 2019.

[2] Q. Wu and R. Zhang, "Towards smart and reconfigurable environment: Intelligent reflecting surface aided wireless network," *IEEE Communications Magazine*, vol. 58, no. 1, pp. 106–112, 2020.

[3] M. Di Renzo, K. Ntontin, J. Song, F. H. Danufane, X. Qian, F. Lazarakis, J. De Rosny, D.-T. Phan-Huy, O. Simeone, R. Zhang, M. Debbah, G. Lerosey, M. Fink, S. Tretyakov, and S. Shamai, "Reconfigurable intelligent surfaces vs. relaying: Differences, similarities, and performance comparison," *IEEE Open Journal of the Communications Society*, vol. 1, pp. 798–807, 2020.

[4] L. Dai, B. Wang, M. Wang, X. Yang, J. Tan, S. Bi, S. Xu, F. Yang, Z. Chen, M. D. Renzo, C.-B. Chae, and L. Hanzo, "Reconfigurable intelligent surface-based wireless communications: Antenna design, prototyping, and experimental results," *IEEE Access*, vol. 8, pp. 45 913–45 923, 2020.

[5] Z. Zhang, L. Dai, X. Chen, C. Liu, F. Yang, R. Schober, and H. V. Poor, "Active ris vs. passive ris: Which will prevail in 6g?" *IEEE Transactions on Communications*, vol. 71, no. 3, pp. 1707–1725, 2023.

[6] C. Huang, A. Zappone, G. C. Alexandropoulos, M. Debbah, and C. Yuen, "Reconfigurable intelligent surfaces for energy efficiency in wireless communication," *IEEE Transactions on Wireless Communications*, vol. 18, no. 8, pp. 4157–4170, 2019.

[7] J. Ye, S. Guo, and M.-S. Alouini, "Joint reflecting and precoding designs for ser minimization in reconfigurable intelligent surfaces assisted mimo systems," *IEEE Transactions on Wireless Communications*, vol. 19, no. 8, pp. 5561–5574, 2020.

[8] R. Y. Mesleh, H. Haas, S. Sinanovic, C. W. Ahn, and S. Yun, "Spatial modulation," *IEEE Transactions on Vehicular Technology*, vol. 57, no. 4, pp. 2228–2241, 2008.

[9] E. Basar, "Reconfigurable intelligent surface-based index modulation: A new beyond mimo paradigm for 6g," *IEEE Transactions on Communications*, vol. 68, no. 5, pp. 3187–3196, 2020.

[10] S. Luo, P. Yang, Y. Che, K. Yang, K. Wu, K. C. Teh, and S. Li, "Spatial modulation for ris-assisted uplink communication: Joint power allocation and passive beamforming design," *IEEE Transactions on Communications*, vol. 69, no. 10, pp. 7017–7031, 2021.

[11] K. Asmoro and S. Y. Shin, "Ris grouping based index modulation for 6g telecommunications," *IEEE Wireless Communications Letters*, vol. 11, no. 11, pp. 2410–2414, 2022.

[12] P. Cheng, Z. Chen, J. A. Zhang, Y. Li, and B. Vucetic, "A unified precoding scheme for generalized spatial modulation," *IEEE Transactions on Communications*, vol. 66, no. 6, pp. 2502–2514, 2018.

[13] P. Yang, Y. L. Guan, Y. Xiao, M. D. Renzo, S. Li, and L. Hanzo, "Transmit precoded spatial modulation: Maximizing the minimum euclidean distance versus minimizing the bit error ratio," *IEEE Transactions on Wireless Communications*, vol. 15, no. 3, pp. 2054–2068, 2016.

[14] M. Grant and S. Boyd, "CVX: Matlab software for disciplined convex programming, version 2.1," http://cvxr.com/cvx, Mar. 2014.

[15] ——, "Graph implementations for nonsmooth convex programs," in *Recent Advances in Learning and Control*, ser. Lecture Notes in Control and Information Sciences, V. Blondel, S. Boyd, and H. Kimura, Eds. Springer-Verlag Limited, 2008, pp. 95–110, http://stanford.edu/ boyd/graph$_{d}cp.html$.